

# I-Perceive: A Foundation Model for Vision-Language Active Perception

Yongxi Huang\*, Zhuohang Wang<sup>†‡</sup>, Wenjing Tang\*, Cewu Lu\*<sup>†</sup>, Panpan Cai\*<sup>†</sup>

\*Shanghai Jiao Tong University {huangyongxi, cai\_panpan}@sjtu.edu.cn

<sup>†</sup>Shanghai Innovation Institute

<sup>‡</sup>Beihang University

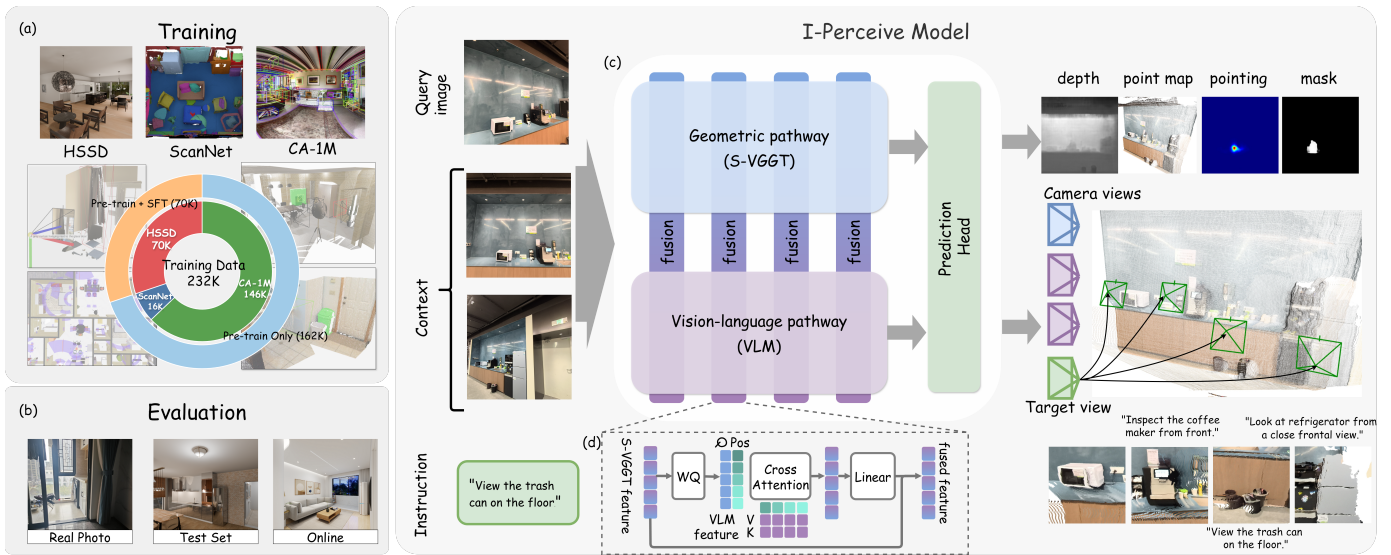


Fig. 1: **I-Perceive** is a foundation model for vision-language active perception. Given context images and a natural language instruction, the model predicts a target camera pose that fulfills the observation intent. By fusing VLM semantic features into a geometric backbone, I-Perceive demonstrates strong zero-shot generalization to unseen real-world environments.

**Abstract**—Active perception, the ability of a robot to proactively adjust its viewpoint to acquire task-relevant information, is essential for robust operation in unstructured real-world environments. While critical for downstream tasks such as manipulation, existing approaches have largely been confined to local settings (e.g., table-top scenes) with fixed perception objectives (e.g., occlusion reduction). Addressing active perception with open-ended intents in large-scale environments remains an open challenge. To bridge this gap, we propose I-Perceive, a foundation model for active perception conditioned on natural language instructions, designed for mobile manipulators and indoor environments. I-Perceive predicts camera views that follows open-ended language instructions, based on image-based scene contexts. By fusing a Vision-Language Model (VLM) backbone with a geometric foundation model, I-Perceive bridges semantic and geometric understanding, thus enabling effective reasoning for active perception. We train I-Perceive on a diverse dataset comprising real-world scene-scanning data and simulation data, both processed via an automated and scalable data generation pipeline. Experiments demonstrate that I-Perceive significantly outperforms state-of-the-art VLMs in both prediction accuracy and instruction following of generated camera views, and exhibits strong zero-shot generalization to novel scenes and tasks.

## I. INTRODUCTION

Active perception refers to a robot’s ability to proactively control its camera pose in order to acquire task-relevant information for downstream decision-making and execution. Existing approaches, however, are largely fragmented. On the one hand, many methods are designed for fixed downstream tasks—such as object detection, pose estimation, or scene reconstruction—where the perception objective is hard-coded into task-specific optimization losses. As a result, models developed for different tasks are isolated, difficult to integrate, and lack generality. On the other hand, a large body of work assumes highly constrained environments, typically limited to table-top or small-scale scenes, which restricts their applicability to real-world indoor settings.

In this work, we aim to provide a foundation model for active perception that overcomes these limitations, allowing (1) generalizing to open-ended perception intents specified by natural language instructions, and (2) scaling to large-scale indoor environments suitable for mobile manipulators. Achieving this goal poses several fundamental challenges. First, the model must infer perception intent from natural language instructions, which are inherently diverse and

underspecified. Second, it must recover the geometry of large scenes from sparse visual observations, bridging the gap from image space (2D) to geometry space (3D). Third, it must ground language-specified intents into the visual and geometric representations of the scene, requiring alignment across language, image, and geometry spaces. Finally, the model must transform the geometry of task-relevant regions or objects into actionable camera poses, mapping 3D scene understanding to 6D camera poses.

Recent advances offer partial solutions to these challenges. Vision-Language Models (VLMs) have demonstrated strong capability in aligning language with visual observations, while geometric foundation models such as VGGT enable mapping from images to 3D geometry and camera poses. However, language has not yet been successfully integrated into camera view decision-making for active perception, leaving a critical gap between instruction understanding and viewpoint control.

To fill this gap, we propose I-Perceive, a foundation model for active perception that predicts camera viewpoints conditioned on natural language instructions in large-scale indoor environments. Given a query image and a set of context images capturing the surrounding scene, I-Perceive takes an open-ended language instruction specifying a perception intent and outputs a desirable 6D camera pose that fulfills the instruction. I-Perceive is built upon two complementary foundations: a Vision-Language Model (VLM) backbone for language-vision grounding, and a VGGT-based geometric grounding model for 3D scene understanding and camera pose reasoning. However, while these components individually address language alignment and geometric reasoning, directly combining them is insufficient for instruction-driven viewpoint decision-making.

To this end, we introduce two crucial architectural modifications. First, we introduce *semantic fusion layers* to explicitly connect the VLM backbone with the VGGT backbone via cross-attention, enabling the language-grounded visual semantics to be injected into the geometric reasoning pathway, guiding how candidate camera viewpoints are evaluated. Building on this principle, we develop *Semantic VGGT (S-VGGT)*, a semantic-aware extension of VGGT in which semantically-fused features are propagated alongside geometric features through alternative layers of global and intra-frame attentions. This design embeds semantic intent throughout the geometric reasoning process, resulting in camera pose predictions that are jointly informed by *what the instruction asks for* and *how the scene is structured in 3D*.

To train I-Perceive on a scale, we constructed a large-scale dataset comprising 162K perception tasks generated from real-world indoor scene-scanning datasets and 70K tasks generated from simulated indoor environments. The real-world scanning tasks are only used for pretraining to promote robust generalization, while the simulation tasks are used to improve the instruction-following ability. All tasks are automatically annotated with ground-truth camera viewpoints using a scalable and fully automated data generation pipeline.

In our experiments, we evaluate I-Perceive on both in-

distribution simulation tasks and out-of-distribution real-world tasks. Results show that I-Perceive significantly outperforms state-of-the-art Vision-Language Models in terms of both camera pose prediction accuracy and instruction following of the generated views, while exhibiting strong zero-shot generalization to novel scenes and previously unseen perception intents. Through qualitative studies, we further demonstrate that I-Perceive can handle complex instructions in natural language, rich visual contexts, and partial observability. The model naturally supports a variable number of context images and consistently improves task performance as more context becomes available. Moreover, I-Perceive enables sequential active perception: when executed multiple times in a closed-loop manner, it progressively refines camera viewpoints, producing progressively-refined views over successive perception steps.

## II. RELATED WORK

### A. Active Perception

Active perception refers to an agent’s ability to intelligently control its sensors to acquire task-relevant information. As formulated by Bajcsy [5, 6], an active perceiver must know *why* it wishes to sense, then determine *what*, *how*, and *where* to perceive. This paradigm has motivated extensive research across robotics and computer vision [1, 44].

*a) Reconstruction-Driven Approaches:* A major line of active perception research focuses on 3D reconstruction, where the goal is to maximize geometric completeness. Classical Next-Best-View (NBV) methods employ generate-and-test strategies, selecting viewpoints that reveal the most unknown voxels [11, 39]. Subsequent works adopted information-theoretic metrics to quantify view utility [18, 14], while learning-based approaches predict NBV directly from partial observations [29, 30]. These methods optimize for geometric coverage but lack the semantic understanding to interpret diverse user intents.

*b) Perception-Driven Approaches:* Active perception has been applied to recognition and pose estimation tasks where semantics are also taken into account. Early works integrated sensor planning with object hypothesis generation [17], while deep learning methods such as 3D ShapeNets [41] select views that minimize classification entropy. Others leverage multi-view reasoning for recognition [20] and 6D pose estimation in cluttered scenes [31, 19]. Vision-Language Navigation (VLN) [2, 40, 15] is also related, where agents navigate to language-specified goals. Recent VLN methods leverage foundation model to provide semantic grounding and reasoning capabilities [23, 28, 45, 43]. Although VLN involves viewpoint selection, its focus is on navigation and view planning is still driven by exploring or correlation with goal locations.

*c) Positioning of Our Work:* Existing active perception methods are typically designed for fixed objectives (*e.g.*, reconstruction, recognition) with hard-coded optimization criteria. In contrast, our work targets *instruction-driven* active perception that generalizes across diverse intents specified

in natural language. This requires jointly reasoning about semantic intent, visual context, and 3D geometry—a capability absent in prior approaches.

### B. Vision-Language and Geometry Foundation Models

a) *VLMs and Spatial Understanding*: Vision-Language Models (VLMs) have achieved remarkable success in semantic understanding and reasoning across vision and language modalities [4, 35, 21]. However, recent studies reveal that VLMs struggle with spatial reasoning and 3D geometric understanding [42, 46]. Some works apply VLMs directly to active perception [49, 32, 22], but these typically operate in constrained settings (e.g., table-top scenes) with limited action spaces (e.g., image cropping or zooming), lacking fundamental 3D scene understanding.

b) *Geometric Foundation Models*: Recently, transformer based geometric foundation models [38, 26, 37] have shown impressive capabilities in recovering 3D structure and camera poses from sparse views. By leveraging large-scale training data and powerful attention mechanisms, VGGT [37] achieves robust spatial reasoning across diverse scenes and viewpoints, enabling effective mapping from discrete images to holistic 3D scene understanding and camera pose inference. However, these models focus purely on geometry and lack the semantic grounding to interpret language instructions and reason about task-relevant information.

c) *Bridging Semantics and Geometry*: Emerging research seeks to combine VLM semantics with geometric reasoning. Some works enhance VLMs’ intrinsic spatial understanding through language-level supervision [9, 48, 8]. Another direction integrates explicit geometric features from geometric foundation models into VLMs [27] to do downstream tasks such as manipulation. These works demonstrate the potential of leveraging both VLMs and geometric foundation models for joint semantic-spatial reasoning. Building on this insight, I-Perceive introduces a unified architecture that deeply fuses capabilities of both pretrained model families, enabling instruction-driven active perception that jointly understands *what* the user wants to observe and *where* it is located in 3D space.

## III. OVERVIEW

The I-Perceive model determines where a robot should look—i.e., predicts a camera pose—to fulfill a perception intent specified by a natural language instruction. Given a query image representing the robot’s current view and a set of context images collected along its past trajectory, I-Perceive outputs a target camera pose that best satisfies the instruction in large-scale indoor environments.

At a high level, I-Perceive reasons about camera viewpoint selection through two tightly coupled pathways: a *geometric reasoning pathway* and a *vision-language pathway*. The geometric pathway focuses on 3D scene understanding and camera pose reasoning, modeling spatial relationships across the query, context views, and a placeholder target view whose representation is progressively inferred. In parallel,

the vision-language pathway processes the natural language instruction together with visual inputs to extract semantic intent. Crucially, semantic intent from the language pathway is progressively fused into the geometric pathway at multiple layers, enabling language-conditioned geometric reasoning rather than treating perception and instruction understanding as separate stages.

This design allows I-Perceive to ground open-ended language instructions into both visual observations and 3D scene geometry, and to directly transform the inferred geometry of task-relevant regions into an actionable 6D camera pose. The model jointly predicts camera poses for all observed frames as well as the target frame, and can additionally produce dense geometric and semantic outputs such as depth maps, point maps, pointing heatmaps, and object/region-level semantic masks.

I-Perceive is trained on a large-scale and diverse dataset of perception tasks combining both real-world and simulated data. Real-world tasks are derived from indoor scene-scanning datasets, where meaningful target viewpoints are identified and paired with automatically generated language instructions, and are primarily used for pretraining to encourage robust generalization. Complementary simulation-based tasks are generated in a variety of indoor environments, where target views are programmatically sampled and query–context observations are collected along simulated robot trajectories, and are used for post-training to improve in-domain task performance.

At test time, I-Perceive supports both single-step and sequential active perception. In the sequential setting, the model is executed in a closed-loop manner: it predicts a target view, the robot moves to collect a new observation, and the newly acquired image is incorporated as context for the next prediction. Repeating this process allows I-Perceive to progressively refine camera viewpoints and improve perception quality over time—without additional training or data collection.

The rest of the paper is organized as follows: Section IV-A presents our data generation pipeline, including how we sample tasks, contexts, generate language instructions, and annotate target views. Section IV-B presents the architecture of the I-Perceive model in detail, especially on the structure of our VGGT-like geometric backbone and how VLM features are injected into its reasoning. Section IV-C presents the training tasks and the respective loss functions. Finally, Section V presents both quantitative comparison with state-of-the-art VLMs and qualitative analyses on complex tasks and sequential active perception. We also include a comprehensive failure-mode analysis in Appendix C.

## IV. METHODOLOGY

### A. Data Generation Pipeline

Each training sample consists of a sequence of  $N + 1$  frames  $(\mathcal{F}_i)_{i=0}^N$  and a natural language instruction  $\ell$  specifying an observation intent. The last frame  $\mathcal{F}_N$  is the target frame that fulfills the instruction  $\ell$ , while the first

$N$  frames  $\{\mathcal{F}_i\}_{i=0}^{N-1}$  serve as visual context. Each frame  $\mathcal{F}_i = (I_i, D_i, M_i, \mathbf{g}_i)$  contains an RGB image  $I_i \in \mathbb{R}^{3 \times H \times W}$ , a depth map  $D_i \in \mathbb{R}^{H \times W}$ , a semantic mask  $M_i \in \mathbb{R}^{H \times W}$ , and camera parameters  $\mathbf{g}_i$ . The training data is generated from two sources: real-world indoor scene-scanning datasets (ScanNet [13] and CA-1M [25]) and synthetic scenes dataset (HSSD [24]).

For all data sources, we follow a similar pipeline where we first sample target viewpoints that capture meaningful observations, then collect start and context frames, and finally generate language instructions describing the observation intent using a large language model. The frame sampling and instruction generation strategies for ScanNet and CA-1M are quite straightforward.

- 1) **ScanNet**: Sample candidate viewpoints with annotated object semantic mask at center. Filter out candidates with small visible area. Randomly select one as target. Start and context frames are sampled according to their camera pose. The category label is provided together with target view to LLM for instruction generation.
- 2) **CA-1M**: Similar to ScanNet, but target viewpoint is sampled based on object bounding boxes instead of semantic masks. Frames with a view direction close to object center and aligned with bounding box axis are taken as target frame candidates. CA-1M provides richer object semantic caption, which is used to prompt LLM for instruction generation.

As for synthetic scenes in HSSD, we first annotate a set of “target poses” for each asset model. Each target pose contains a sampling range and an objective description about the pose. During data generation, a bunch of robot trajectories are simulated in the scene with path planning between sampled target poses. The start and context frames are collected after executing the planned trajectory. And the prompt LLM with the objective description and rgb image at start and target poses for instruction generation. The depth and semantic segmentation maps are rendered from the 3D asset model through Genesis [3] and the photo-realistic RGB images are rendered through Blender [7] with manually adjusted lighting settings. See more details in Appendix A. The generated instructions can express various intents, such as:

- **Object category**: “Inspect the cabinet ...”
- **Target identification**: “... above the sink ...”
- **View point description**: “... from an eye-level view ...”
- **Functional**: “... to inspect its contents.”

However, there are cases that the same language instruction can correspond to multiple target objects or regions in the scene. To resolve this ambiguity, we let LLM to decide whether the instruction causes ambiguity, and if so, a 2D point coordinate is added to the instruction in form of “(x, y) in image” to indicate the intended target. Finally, we obtain 162K training samples from ScanNet and CA-1M, and 70K samples from HSSD.

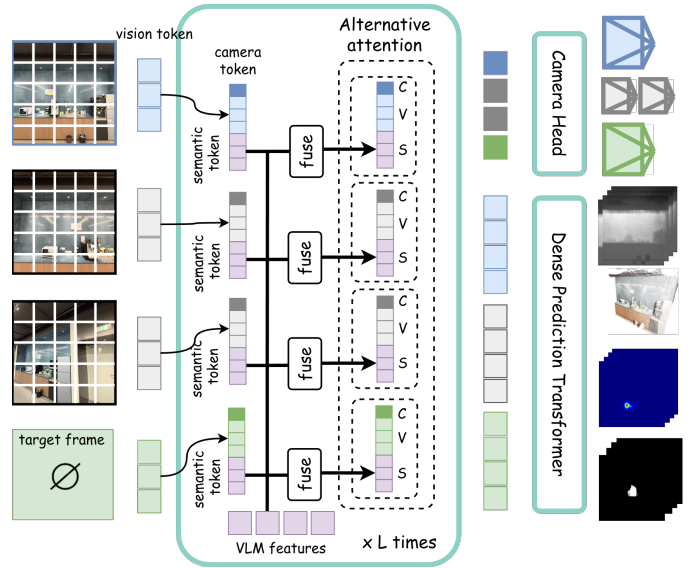


Fig. 2: I-Perceive model architecture. The VLM backbone is not shown in detail for simplicity. Semantic features are extracted from intermediate layers of the VLM and fused into semantic tokens in the S-VGGT geometric backbone.

## B. Model Architecture

The overall architecture, illustrated in Fig. 2, consists of two main components: (1) a VLM backbone that provides semantic understanding of visual and language inputs, and (2) geometry grounding model that integrates geometric reasoning with semantic features to predict target camera poses.

a) *Input and Output*: The model takes as input  $N$  RGB frames  $\{I_i\}_{i=0}^{N-1}$  and a natural language instruction  $\ell$ , where  $I_0$  serves as the start frame establishing the reference coordinate system. The model outputs camera parameters  $\mathbf{g}_N$  for the target view that fulfills the instruction  $\ell$ , along with camera parameters  $\{\mathbf{g}_i\}_{i=0}^{N-1}$  for all input frames. Following VGGT [37], each camera parameter  $\mathbf{g}_i = [\mathbf{q}_i, \mathbf{t}_i, \mathbf{f}_i] \in \mathbb{R}^9$  encodes rotation (quaternion  $\mathbf{q}_i \in \mathbb{R}^4$ ), translation ( $\mathbf{t}_i \in \mathbb{R}^3$ ), and field of view ( $\mathbf{f}_i \in \mathbb{R}^2$ ), all expressed relative to the start frame (i.e.,  $\mathbf{g}_0$  is identity). The model additionally produces depth maps  $D_i \in \mathbb{R}^{H \times W}$  and point maps  $P_i \in \mathbb{R}^{3 \times H \times W}$  for geometric grounding, as well as auxiliary outputs for semantic grounding described in *Output Heads*.

b) *VLM Semantic Feature Extraction*: We use Qwen3-VL [4] directly as our VLM backbone. Given a set of input images  $\mathcal{I} = \{I_i\}_{i=0}^{N-1}$  and a natural language instruction  $\ell$ , we process them through VLM backbone to extract semantic features. Rather than using the final output representations, we extract intermediate key-value (KV) caches from  $N_Q$  selected transformer layers  $\{l_j\}_{j=1}^{N_Q}$  as semantic features:

$$K^{(l_j)}, V^{(l_j)} = \text{ExtractKV}(\text{Qwen3-VL}, l_j, \mathcal{I}, \ell) \quad (1)$$

where  $K^{(l_j)}, V^{(l_j)} \in \mathbb{R}^{B \times H \times L \times D_h}$  denote the key and value tensors from layer  $l_j$ , with  $H$  attention heads, sequence length  $L$ , and head dimension  $D_h$ .

c) *S-VGGT Architecture*: In order to build 3D geometry grounding with semantic understanding, we build a Semantic VGGT (S-VGGT) model based on VGGT [37]. As a feed-forward vision transformer, VGGT build a concatenation of tokens  $(t_i^I, t_i^g, t_i^R)_{i=0}^{N-1}$  for each image frame, where  $t_i^I$  is vision tokens for dense estimation,  $t_i^g$  is camera token for camera parameter regression, and  $t_i^R$  is register token. Our task differs from VGGT in two aspects: (1) we need to incorporate language instruction for semantic understanding, and (2) we need to predict the target camera pose based on the instruction. We introduce two key modifications to the original VGGT architecture.

**Semantic tokens**: We add semantic tokens  $t_i^S \in \mathbb{R}^{P \times C}$  for each image frame to fuse the VLM semantic features into the geometric reasoning process, where  $P$  is the number of image grid patches and  $C$  is the embedding dimension. Similar to the camera and register tokens, semantic tokens are initialized with two set of learnable parameters and repeated to match the patch grid size for each frame.

**Target Frame**: We append a target frame  $I_N$  as a padding frame to represent the unknown target view. It’s vision token is constructed from a learnable token  $t^{\text{pad}} \in \mathbb{R}^C$ , which is repeated to match the patch grid size. Other tokens are constructed just like context frames.

The overall token structure per frame becomes  $(t_i^I, t_i^g, t_i^R, t_i^S)_{i=0}^N$ , which is then passed to the alternating attention blocks for multi-view aggregation. The target frame  $i = N$  serves as a dummy frame just like other image frames, allowing the model to reason about the target view in conjunction with context views. Through cross-attention with semantic features from the VLM, semantic tokens carry language-grounded information that informs geometric reasoning throughout the network.

d) *Semantic Fusion*: As shown in Fig. 1 (d), we fuse VLM semantic features into S-VGGT through cross-attention at  $N_Q$  selected layers  $\{l_k\}_{k=1}^{N_Q}$  within the alternating attention blocks. At fusion layer  $k$ , semantic tokens serve as queries to attend over VLM KV features:

$$t_i^{S'} = t_i^S + \gamma \cdot \text{Proj}_{\text{out}}(\text{Attn}(W_Q t_i^S, K., V.)) \quad (2)$$

where  $W_Q$  projects S-VGGT features to the VLM dimension,  $\text{Proj}_{\text{out}}$  projects back to S-VGGT dimension, and  $\gamma \in \mathbb{R}^C$  is a learnable linear scaler initialized to zero for training stability. The VLM KV features  $(K., V.)$  depend on the frame type and position. For image frames  $i \in [0, N - 1]$ , we use image KV features from corresponding spatial locations in  $K^{(l_j)}, V^{(l_j)}$ . A relative 2D rotary position embeddings (RoPE) [33] is applied to both queries and keys to preserve spatial correspondence. For the target frame  $i = N$ , we use instruction KV features from  $K^{(l_j)}, V^{(l_j)}$  with 1D RoPE applied only to keys. This asymmetric design reflects that instruction semantics should be spatially invariant when projected onto the target frame.

e) *Output Heads*: S-VGGT preserves the original VGGT prediction heads for camera pose, depth, and 3D points. The camera head processes aggregated tokens to output

pose encodings, which are decoded into extrinsic camera parameters. Additionally, we add auxiliary heads for point instruction understanding (predicting the point occurs in instruction as heatmaps of every frame) and semantic masks (dense segmentation for target object in every frame), which provide supervisory signals that encourage the model to encode task-relevant semantics during training.

### C. Training

We first pre-train I-Perceive on data from all three datasets (ScanNet, CA-1M, HSSD) with VLM backbone frozen and all learning targets enabled for 5 epochs. Then we fine-tune the model on HSSD data only, unfreezing VLM backbone with LoRA [16] and disabling semantic mask and point heatmap losses to focus on instruction following for 1 epoch. The training process takes 25 hours on 32 H200 GPUs.

## V. EXPERIMENTS

We evaluate I-Perceive on diverse indoor scenes to assess its ability to generate appropriate camera poses for various observation intents. Our experiments aim to answer the following questions: (1) Can I-Perceive generalize to novel scenes and camera configurations not seen during training? (2) How does I-Perceive compare to state-of-the-art vision-language models on active perception tasks? (3) Do the generated camera poses align with human judgment of task completion?

### A. Experimental Setup

a) *Evaluation Tasks*: The quantitative evaluation is conducted on a held-out test set of 270 samples from HSSD with unseen scenes during training. Instead of using the data generation pipeline to annotate target views, we manually annotate target viewpoints to ensure high-quality and unambiguous observation intents.

We also perform qualitative evaluation on photos captured by mobile cameras in real-world indoor environments and rendered images from online interior design platform Coohom [12] to test zero-shot generalization of I-Perceive.

b) *Baselines*: We compare I-Perceive against three strong vision-language models: GPT-5.2, Gemini3-Pro, and Qwen3-VL [4], prompted to output camera pose parameters given the visual context and instruction. We use the public APIs for GPT-5.2 and Gemini3-Pro, and a local deployment for Qwen3-VL-235B-A22B-Instruct. The camera pose is represented as a textual description of camera location and look-at point on image coordinates when evaluating VLM baselines, which is friendly to VLMs.

c) *Evaluation Metrics*: Evaluating active perception is inherently challenging due to the subjective nature of observation intents. We employ both geometric metrics that measure alignment with ground-truth poses and preference-based metrics that assess task completion quality.

**View Coverage IoU**. We utilize the volumetric IoU of visible voxels to quantify the effectiveness of active perception, which is commonly used to measure the similarity

or coverage of viewpoints in 3D reconstruction and next-best-view planning [18, 10, 30]. Given a voxelized scene representation  $\mathcal{V}$ , we compute the set of visible voxels  $\mathcal{V}(\mathbf{g})$  for a camera with parameters  $\mathbf{g}$  through frustum culling and visibility testing. The View Coverage IoU is then defined as:

$$\text{IoU} = \frac{|\mathcal{V}(\mathbf{g}_{\text{pred}}) \cap \mathcal{V}(\mathbf{g}_{\text{gt}})|}{|\mathcal{V}(\mathbf{g}_{\text{pred}}) \cup \mathcal{V}(\mathbf{g}_{\text{gt}})|}. \quad (3)$$

This metric captures whether the predicted viewpoint observes similar scene content as the ground-truth, which is more semantically meaningful than raw pose error for active perception tasks.

**Camera Pose Error.** We separately report translation and rotation errors to provide interpretable pose accuracy measures. The translation error is the Euclidean distance between camera centers and the rotation error is the geodesic distance on  $SO(3)$ .

**Judge Ranking.** Given the subjective nature of active perception—where multiple viewpoints might satisfy an instruction to varying degrees—we adopt a Listwise Ranking evaluation protocol, inspired by LLM-as-a-Judge benchmarks [34, 47]. Instead of pairwise comparisons, we present the judge with the visual context, the language instruction, and the set of views generated by all competing methods (including the Ground Truth) simultaneously. The judge is then prompted to rank the views from best to worst based on instruction fulfillment and visibility. We employ two state-of-the-art foundation models as judges, **GPT-5.2** and **Gemini3-Pro**, to mitigate single-model bias. We conduct this evaluation on  $N = 270$  test samples. To eliminate position bias, we perform multiple permutations of the candidate order for each sample and report the Mean Rank (lower is better). Detailed prompting strategies and permutation settings are provided in Appendix B.

Besides VLM judges, we also conduct human evaluation to assess alignment with human judgment. We conduct a human evaluation on a randomly sampled subset of 50 tasks from the test set. Human annotators are presented with the same anonymized candidate views and asked to rank them based on how well they satisfy the observation intent.

### B. Quantitative Results

Table I and Table II present quantitative comparisons on geometric and preference-based metrics, respectively. I-Perceive consistently outperforms all baselines on both evaluation dimensions.

*a) Geometric Performance:* As shown in Table I, I-Perceive achieves a View Coverage IoU of 46.8%, significantly outperforming the best baseline (Gemini3-Pro) by 11.7%. This indicates that I-Perceive generates viewpoints that observe substantially more relevant scene content aligned with the observation intent. Additionally, I-Perceive attains the lowest translation error (0.85 m) and rotation error (0.50 rad), demonstrating superior pose accuracy compared to baselines.

The results also highlight the limitations of directly prompting VLMs for camera pose generation. As these general

TABLE I: Geometric evaluation results. We report View Coverage IoU (%), translation error  $e_t$  (m), and rotation error  $e_r$  (rad).  $\uparrow$ : higher is better;  $\downarrow$ : lower is better.

Method	IoU(%) $\uparrow$	$e_t$ (m) $\downarrow$	$e_r$ (rad) $\downarrow$
<i>VLMs w/o Spatial Prompt</i>			
GPT-5.2	26.2	1.45	0.97
Qwen3-VL	6.20	2.58	2.01
Gemini3-Pro	35.1	1.23	0.68
<i>VLMs w/ Spatial Prompt</i>			
GPT-5.2	24.0	1.48	0.98
Qwen3-VL	9.16	1.81	2.08
Gemini3-Pro	34.3	1.28	0.70
<b>I-Perceive</b>	<b>46.8</b>	<b>0.85</b>	<b>0.50</b>

TABLE II: Preference-based evaluation. We report Mean Rank (lower is better) assigned by VLM judges (GPT-5.2, Gemini3-Pro) and human annotators.

Method	GPT Rank $\downarrow$	Gemini Rank $\downarrow$	Human Rank $\downarrow$
GPT-5.2	3.58	3.59	3.66
Qwen3-VL	4.28	4.47	4.30
Gemini3-Pro	2.95	3.01	3.32
<b>I-Perceive</b>	2.56	2.34	2.18
Human	1.64	1.61	1.54

models are not explicitly trained for geometric reasoning, they struggle to infer accurate viewpoints solely from language and image inputs. In that case, we try to provide spatial prompts (the depth value of one point at the target area in start frame) to help VLMs better understand the 3D structure of the scene. However, the improvements are marginal at best, with some metrics even degrading slightly. This suggests that VLMs have difficulty internalizing geometric reasoning purely through language cues. In contrast, I-Perceive’s explicit integration of geometric foundation models enables effective spatial understanding and viewpoint generation.

*b) Preference-Based Evaluation:* As shown in Table II, I-Perceive achieves the second lowest Mean Rank across both VLM judges and human judges, just behind the ground truth views annotated by humans. This demonstrates that I-Perceive’s generated viewpoints are consistently preferred over those from baseline VLMs, indicating its superior ability to generate viewpoints that align with observation intents. Notably, the rankings assigned by VLM judges exhibit a high correlation with human judgments, validating the reliability of using foundation models as evaluators in this context.

### C. Qualitative Generalization

*a) Comparison with Baselines:* Fig. 3 presents qualitative comparisons between I-Perceive and VLM baselines on diverse test samples. I-Perceive consistently generates target views that better fulfill the observation intents. It shows our model’s ability to

- Infer the target object or region specified in the instruction. Fig. 3 (a) shows its basic capability of understanding language instruction of the perception target, while (b) demonstrates its ability to use 2D point instruction to resolve ambiguity.

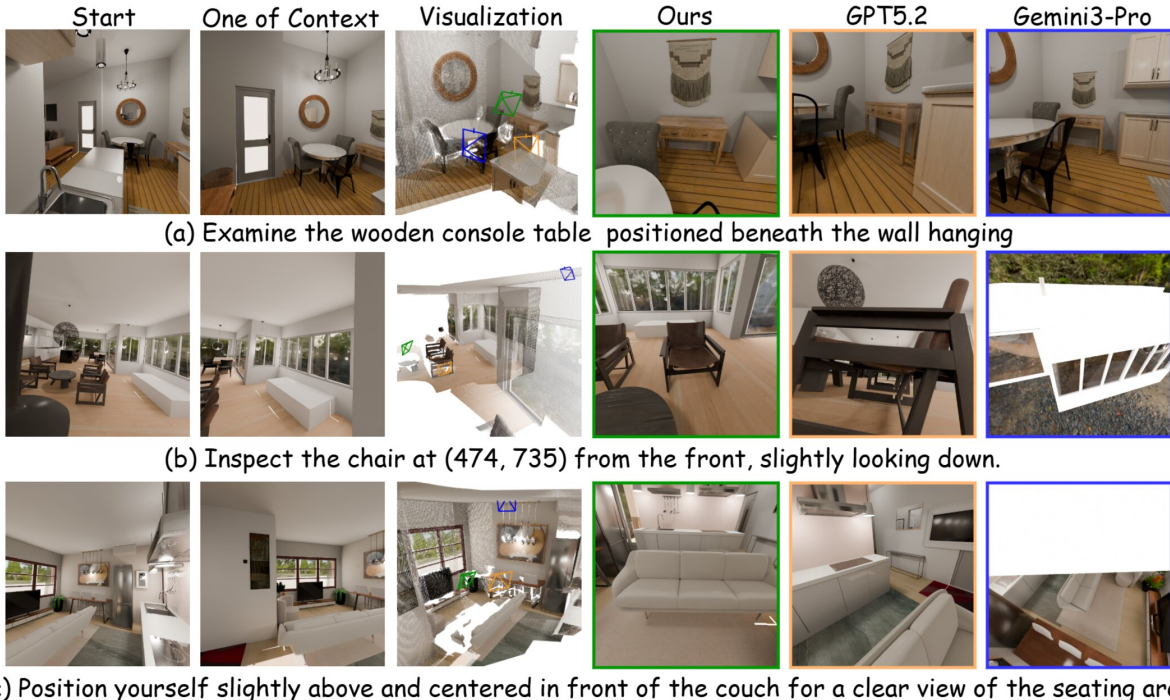


Fig. 3: Qualitative results of I-Perceive and VLM baselines on our test set. The start frame and one context frame are shown on the left, with the language instruction at the bottom. The predicted target views from different methods are visualized by different colored frustums in 3D space and their corresponding rendered RGB images.

- Determine appropriate viewpoints that capture the target effectively. In (a), I-Perceive generates a view that comfortably captures the “console table” from a human-like perspective. In (c), it strictly follows the view direction in the instruction to observe the “couch”.

b) *Zero-Shot Generalization*: Fig. 4 showcases I-Perceive’s zero-shot generalization to real-world indoor photos captured by mobile cameras and rendered images from Coohom [12]. Each example contains two different language instructions with the same visual context, demonstrating I-Perceive’s instruction following ability in novel settings. Despite being trained solely on synthetic and scanned indoor datasets, I-Perceive effectively interprets observation intents and generates appropriate target viewpoints in these novel settings. This highlights the robustness of our approach and its potential applicability to real-world robotic perception tasks.

c) *Closed-Loop Active Perception*: Fig. 5 illustrates I-Perceive operating in a closed-loop active perception setting. Note that the target object “coffee maker” is initially out of view in the start frame. I-Perceive successfully predicts a new viewpoint to the counter area where it is likely to be located. After moving to the predicted view and push last observation back to I-Perceive as visual context, the model further refines its prediction to center the coffee maker in the frame, effectively fulfilling the observation intent.

It is worth noting that I-Perceive is not explicitly trained for closed-loop operation. By training with all geometry grounding tasks and camera pose prediction jointly, I-Perceive learns to build a comprehensive 3D understanding of the scene from sparse views. This capability enables it to reason

about unseen areas and generate viewpoints that progressively improve observation quality through iterative feedback.

#### D. Ablation Studies

To validate the contributions of our key architectural components, we conduct ablation studies on the test set. We analyze the impact of the VLM backbone, the auxiliary supervision tasks, and the deep semantic fusion mechanism. The quantitative results are summarized in Table III.

a) *Effect of VLM Backbone*: A core premise of I-Perceive is that large-scale Vision-Language Models provide superior semantic understanding for open-ended instructions compared to standard encoders. To test this, we simply remove the VLM backbone, replaced by a simple SigLIP2 [36] encoder to provide language feature only. The result (1) in Table III shows a significant performance drop across all metrics, confirming that the rich reasoning priors embedded in the pretrained VLM are essential for interpreting complex instructions and effectively guiding the geometric grounding process.

b) *Effect of Dense Estimation Tasks*: Our model is trained with VGGT prediction heads except the point track

TABLE III: Ablation studies on model components. We report View Coverage IoU (%), translation error  $e_t$  (m), and rotation error  $e_r$  (rad). Best results are bolded.

Model Variant	IoU (%) $\uparrow$	$e_t$ (m) $\downarrow$	$e_r$ (rad) $\downarrow$
1) w/o VLM Backbone	12.7	2.00	1.20
2) w/o Dense Tasks	41.8	0.84	0.43
3) Single Fusion Layer	37.9	0.97	0.53
4) Linear Fusion	41.1	1.10	0.58
<b>I-Perceive (Full)</b>	<b>46.8</b>	<b>0.85</b>	<b>0.50</b>



Fig. 4: (a) Real photos captured by mobile cameras in indoor environments. (b) Rendered images from Coohom. Input frames are shown on the left with language instructions at the bottom. Predicted target views for different instruction is visualized by colored frustums in 3D space along with their rendered RGB images on the right. The rendered RGB images are directly obtained by projecting the dense point cloud estimation from S-VGGT on the predicted target views.

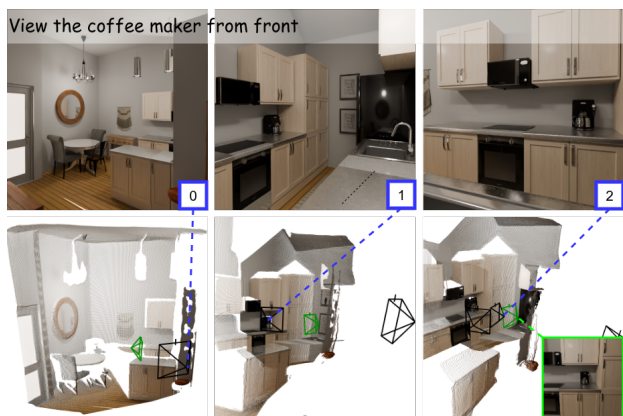


Fig. 5: Calling I-Perceive in closed-loop manner. The first row shows the RGB images captured at each step and the second row visualizes the current target poses prediction as green frustums in 3D space.

head. In this experiment, we only keep the camera pose head. All other dense prediction heads such as depth, point cloud, semantic mask, and point heatmap heads are removed during training. As shown in Row 2 of Table III, the notable performance drop indicates that auxiliary dense prediction tasks help the model better understand the 3D structure of the scene and improve viewpoint reasoning.

*c) Effect of Semantic Fusion:* Our S-VGGT architecture injects semantic information into the geometric reasoning pathway via multiple semantic fusion layers. We evaluate the importance of this design by replacing it with two simpler alternatives:

- A single fusion layer before the first alternating attention block with semantic features from the last VLM layer.
- Four linear projection that directly adds pooled VLM features to the corresponding semantic tokens without

spatial alignment, applied between the same set of layers.

Both variants lead to performance degradation, while the single fusion layer shows a larger drop as shown in Rows 3 and 4 of Table III. This highlights the necessity of deep and spatial aware integration of semantic features throughout the geometric reasoning process to effectively ground language instructions and semantic context into 3D spatial understanding.

## VI. CONCLUSION

We present I-Perceive, an active vision-language perception model that integrates large-scale vision-language models with geometric foundation models to generate target camera poses based on visual context and natural language instructions. Through extensive experiments, we demonstrate I-Perceive’s superior performance over state-of-the-art vision-language models in both geometric accuracy and preference-based evaluations. Our ablation studies validate the contributions of key architectural components, including the VLM backbone and deep semantic fusion mechanism. Qualitative results further showcase I-Perceive’s ability to generalize to real-world settings and operate in closed-loop active perception scenarios. Overall, I-Perceive represents a significant step towards enabling robots to perform instruction-guided active perception in complex environments.

**Limitations and Future Work.** I-Perceive does not consider collision checking or reachability, potentially producing infeasible poses for real robots. This can be resolved by integration with motion planning. Additionally, our dual-pathway architecture relies on two separate pretrained backbones; future work may explore unified multimodal models that jointly learn vision, language, and 3D geometry for tighter integration. Finally, integrating I-Perceive with

downstream robotic systems for end-to-end task execution remains a promising direction.

#### REFERENCES

- [1] John Aloimonos, Isaac Weiss, and Amit Bandyopadhyay. Active vision. *International journal of computer vision*, 1(4):333–356, 1988.
- [2] Peter Anderson, Qi Wu, Damien Teney, Jake Bruce, Mark Johnson, Niko Sünderhauf, Ian Reid, Stephen Gould, and Anton Van Den Hengel. Vision-and-language navigation: Interpreting visually-grounded navigation instructions in real environments. In *Proceedings of the IEEE conference on computer vision and pattern recognition*, pages 3674–3683, 2018.
- [3] Genesis Authors. Genesis: A generative and universal physics engine for robotics and beyond, December 2024. URL <https://github.com/Genesis-Embodied-AI/Genesis>.
- [4] Shuai Bai, Yuxuan Cai, Ruizhe Chen, Keqin Chen, Xionghui Chen, Zesen Cheng, Lianghao Deng, Wei Ding, Chang Gao, Chunjiang Ge, Wenbin Ge, Zhifang Guo, Qidong Huang, Jie Huang, Fei Huang, Binyuan Hui, Shutong Jiang, Zhaohai Li, Mingsheng Li, Mei Li, Kaixin Li, Zicheng Lin, Junyang Lin, Xuejing Liu, Jiawei Liu, Chenglong Liu, Yang Liu, Dayiheng Liu, Shixuan Liu, Dunjie Lu, Ruilin Luo, Chenxu Lv, Rui Men, Lingchen Meng, Xuancheng Ren, Xingzhang Ren, Sibao Song, Yuchong Sun, Jun Tang, Jianhong Tu, Jianqiang Wan, Peng Wang, Pengfei Wang, Qiuyue Wang, Yuxuan Wang, Tianbao Xie, Yiheng Xu, Haiyang Xu, Jin Xu, Zhibo Yang, Mingkun Yang, Jianxin Yang, An Yang, Bowen Yu, Fei Zhang, Hang Zhang, Xi Zhang, Bo Zheng, Humen Zhong, Jingren Zhou, Fan Zhou, Jing Zhou, Yuanzhi Zhu, and Ke Zhu. Qwen3-vl technical report. *arXiv preprint arXiv:2511.21631*, 2025.
- [5] Ruzena Bajcsy. Active perception. *Proceedings of the IEEE*, 76(8):966–1005, 1988.
- [6] Ruzena Bajcsy, Yiannis Aloimonos, and John K Tsotsos. Revisiting active perception. *Autonomous Robots*, 42(2): 177–196, 2018.
- [7] Blender Online Community. Blender - a 3d modelling and rendering package, 2025. URL <http://www.blender.org>.
- [8] Meng Cao, Xingyu Li, Xue Liu, Ian Reid, and Xiaodan Liang. Spatialdreamer: Incentivizing spatial reasoning via active mental imagery. *arXiv preprint arXiv:2512.07733*, 2025.
- [9] Boyuan Chen, Zhuo Xu, Sean Kirmani, Brain Ichter, Dorsa Sadigh, Leonidas Guibas, and Fei Xia. Spatialvlm: Endowing vision-language models with spatial reasoning capabilities. In *Proceedings of the IEEE/CVF Conference on Computer Vision and Pattern Recognition*, pages 14455–14465, 2024.
- [10] Ricson Cheng, Ziyang Wang, and Katerina Fragkiadaki. Geometry-aware recurrent neural networks for active visual recognition. *Advances in Neural Information Processing Systems*, 31, 2018.
- [11] Cl Connolly. The determination of next best views. In *Proceedings. 1985 IEEE international conference on robotics and automation*, volume 2, pages 432–435. IEEE, 1985.
- [12] Coohom Inc. Coohom: Cloud-based 3d rendering and interior design tool. <https://www.coohom.com>, 2026. Accessed: 2026-01-30.
- [13] Angela Dai, Angel X Chang, Manolis Savva, Maciej Halber, Thomas Funkhouser, and Matthias Nießner. Scannet: Richly-annotated 3d reconstructions of indoor scenes. In *Proceedings of the IEEE conference on computer vision and pattern recognition*, pages 5828–5839, 2017.
- [14] Jeffrey Delmerico, Stefan Isler, Reza Sabzevari, and Davide Scaramuzza. A comparison of volumetric information gain metrics for active 3d object reconstruction. *Autonomous Robots*, 42(2):197–208, 2018.
- [15] Yicong Hong, Qi Wu, Yuankai Qi, Cristian Rodriguez-Opazo, and Stephen Gould. Vln bert: A recurrent vision-and-language bert for navigation. In *Proceedings of the IEEE/CVF conference on Computer Vision and Pattern Recognition*, pages 1643–1653, 2021.
- [16] Edward J Hu, Yelong Shen, Phillip Wallis, Zeyuan Allen-Zhu, Yuanzhi Li, Shean Wang, Lu Wang, and Weizhu Chen. LoRA: Low-rank adaptation of large language models. In *International Conference on Learning Representations*, 2022. URL <https://openreview.net/forum?id=nZeVKeeFYf9>.
- [17] Seth A Hutchinson, Robert L Cromwell, and Avinash C Kak. Planning sensing strategies in a robot work cell with multi-sensor capabilities. In *Proceedings. 1988 IEEE International Conference on Robotics and Automation*, pages 1068–1075. IEEE, 1988.
- [18] Stefan Isler, Reza Sabzevari, Jeffrey Delmerico, and Davide Scaramuzza. An information gain formulation for active volumetric 3d reconstruction. In *2016 IEEE International Conference on Robotics and Automation (ICRA)*, pages 3477–3484. IEEE, 2016.
- [19] Snehal Jauhri, Sophie Lueth, and Georgia Chalvatzaki. Active-perceptive motion generation for mobile manipulation. In *2024 IEEE International Conference on Robotics and Automation (ICRA)*, pages 1413–1419. IEEE, 2024.
- [20] Edward Johns, Stefan Leutenegger, and Andrew J Davison. Pairwise decomposition of image sequences for active multi-view recognition. In *Proceedings of the IEEE conference on computer vision and pattern recognition*, pages 3813–3822, 2016.
- [21] Siddharth Karamcheti, Suraj Nair, Ashwin Balakrishna, Percy Liang, Thomas Kollar, and Dorsa Sadigh. Prismatic vlms: Investigating the design space of visually-conditioned language models. In *Forty-first International Conference on Machine Learning*, 2024.
- [22] Justin Kerr, Kush Hari, Ethan Weber, Chung Min Kim, Brent Yi, Tyler Bonnen, Ken Goldberg, and Angjoo

- Kanazawa. Eye, robot: Learning to look to act with a bc-rl perception-action loop. *arXiv preprint arXiv:2506.10968*, 2025.
- [23] Apoorv Khandelwal, Luca Weihs, Roozbeh Mottaghi, and Aniruddha Kembhavi. Simple but effective: Clip embeddings for embodied ai. In *Proceedings of the IEEE/CVF Conference on Computer Vision and Pattern Recognition*, pages 14829–14838, 2022.
- [24] Mukul Khanna\*, Yongsun Mao\*, Hanxiao Jiang, Sanjay Haresh, Brennan Shacklett, Dhruv Batra, Alexander Clegg, Eric Undersander, Angel X. Chang, and Manolis Savva. Habitat Synthetic Scenes Dataset (HSSD-200): An Analysis of 3D Scene Scale and Realism Tradeoffs for ObjectGoal Navigation. *arXiv preprint*, 2023.
- [25] Justin Lazarow, David Griffiths, Gefen Kohavi, Francisco Crespo, and Afshin Dehghan. Cubify anything: Scaling indoor 3d object detection. In *Proceedings of the Computer Vision and Pattern Recognition Conference*, pages 22225–22233, 2025.
- [26] Vincent Leroy, Johann Cabon, and Jérôme Revaud. Grounding image matching in 3d with mast3r. In *European Conference on Computer Vision*, pages 71–91. Springer, 2024.
- [27] Tao Lin, Gen Li, Yilei Zhong, Yanwen Zou, Yuxin Du, Jiting Liu, Encheng Gu, and Bo Zhao. Evo-0: Vision-language-action model with implicit spatial understanding. *arXiv preprint arXiv:2507.00416*, 2025.
- [28] Arjun Majumdar, Gunjan Aggarwal, Bhavika Devnani, Judy Hoffman, and Dhruv Batra. Zson: Zero-shot object-goal navigation using multimodal goal embeddings. *Advances in Neural Information Processing Systems*, 35: 32340–32352, 2022.
- [29] Miguel Mendoza, J Irving Vasquez-Gomez, Hind Taud, L Enrique Sucar, and Carolina Reta. Supervised learning of the next-best-view for 3d object reconstruction. *Pattern Recognition Letters*, 133:224–231, 2020.
- [30] Daryl Peralta, Joel Casimiro, Aldrin Michael Nilles, Justine Aletta Aguilar, Rowel Atienza, and Rhandley Cajote. Next-best view policy for 3d reconstruction. In *European Conference on Computer Vision*, pages 558–573. Springer, 2020.
- [31] Juil Sock, S Hamidreza Kasaei, Luis Seabra Lopes, and Tae-Kyun Kim. Multi-view 6d object pose estimation and camera motion planning using rgbd images. In *Proceedings of the IEEE International Conference on Computer Vision Workshops*, pages 2228–2235, 2017.
- [32] Venkatesh Sripada, Samuel Carter, Frank Guerin, and Amir Ghalamzan. Ap-vlm: Active perception enabled by vision-language models. *arXiv preprint arXiv:2409.17641*, 2024.
- [33] Jianlin Su, Murtadha Ahmed, Yu Lu, Shengfeng Pan, Wen Bo, and Yunfeng Liu. Roformer: Enhanced transformer with rotary position embedding. *Neurocomputing*, 568:127063, 2024.
- [34] Weiwei Sun, Lingyong Yan, Xinyu Ma, Pengjie Ren, Dawei Yin, and Zhaochun Ren. Is chatgpt good at search? investigating large language models as re-ranking agent. *ArXiv*, abs/2304.09542, 2023.
- [35] Gemini Team, Rohan Anil, Sebastian Borgeaud, Jean-Baptiste Alayrac, Jiahui Yu, Radu Soricut, Johan Schalkwyk, Andrew M Dai, Anja Hauth, Katie Millican, et al. Gemini: a family of highly capable multimodal models. *arXiv preprint arXiv:2312.11805*, 2023.
- [36] Michael Tschannen, Alexey Gritsenko, Xiao Wang, Muhammad Ferjad Naeem, Ibrahim Alabdulmohsin, Nikhil Parthasarathy, Talfan Evans, Lucas Beyer, Ye Xia, Basil Mustafa, et al. Siglip 2: Multilingual vision-language encoders with improved semantic understanding, localization, and dense features. *arXiv preprint arXiv:2502.14786*, 2025.
- [37] Jianyuan Wang, Minghao Chen, Nikita Karaev, Andrea Vedaldi, Christian Rupprecht, and David Novotny. Vggt: Visual geometry grounded transformer. In *Proceedings of the Computer Vision and Pattern Recognition Conference*, pages 5294–5306, 2025.
- [38] Shuzhe Wang, Vincent Leroy, Johann Cabon, Boris Chidlovskii, and Jerome Revaud. Dust3r: Geometric 3d vision made easy. In *Proceedings of the IEEE/CVF Conference on Computer Vision and Pattern Recognition*, pages 20697–20709, 2024.
- [39] Laurana M Wong, Christophe Dumont, and Mongi A Abidi. Next best view system in a 3d object modeling task. In *Proceedings 1999 IEEE International Symposium on Computational Intelligence in Robotics and Automation. CIRA'99 (Cat. No. 99EX375)*, pages 306–311. IEEE, 1999.
- [40] Wansen Wu, Tao Chang, Xinmeng Li, Qunjun Yin, and Yue Hu. Vision-language navigation: a survey and taxonomy. *Neural Computing and Applications*, 36(7): 3291–3316, 2024.
- [41] Zhirong Wu, Shuran Song, Aditya Khosla, Fisher Yu, Linguang Zhang, Xiaoou Tang, and Jianxiong Xiao. 3d shapenets: A deep representation for volumetric shapes. In *Proceedings of the IEEE conference on computer vision and pattern recognition*, pages 1912–1920, 2015.
- [42] Jihan Yang, Shusheng Yang, Anjali W Gupta, Rilyn Han, Li Fei-Fei, and Saining Xie. Thinking in space: How multimodal large language models see, remember, and recall spaces. In *Proceedings of the Computer Vision and Pattern Recognition Conference*, pages 10632–10643, 2025.
- [43] Naoki Yokoyama, Sehoon Ha, Dhruv Batra, Jiuguang Wang, and Bernadette Bucher. Vlfm: Vision-language frontier maps for zero-shot semantic navigation. In *2024 IEEE International Conference on Robotics and Automation (ICRA)*, pages 42–48. IEEE, 2024.
- [44] Rui Zeng, Yuhui Wen, Wang Zhao, and Yong-Jin Liu. View planning in robot active vision: A survey of systems, algorithms, and applications. *Computational Visual Media*, 6(3):225–245, 2020.
- [45] Jiazhao Zhang, Kunyu Wang, Rongtao Xu, Gengze Zhou, Yicong Hong, Xiaomeng Fang, Qi Wu, Zhizheng Zhang,

and He Wang. Navid: Video-based vlm plans the next step for vision-and-language navigation. *arXiv preprint arXiv:2402.15852*, 2024.

- [46] Wanyue Zhang, Yibin Huang, Yangbin Xu, JingJing Huang, Helu Zhi, Shuo Ren, Wang Xu, and Jiajun Zhang. Why do mllms struggle with spatial understanding? a systematic analysis from data to architecture. *arXiv preprint arXiv:2509.02359*, 2025.
- [47] Lianmin Zheng, Wei-Lin Chiang, Ying Sheng, Siyuan Zhuang, Zhanghao Wu, Yonghao Zhuang, Zi Lin, Zhuohan Li, Dacheng Li, Eric Xing, et al. Judging llm-as-a-judge with mt-bench and chatbot arena. *Advances in neural information processing systems*, 36:46595–46623, 2023.
- [48] Enshen Zhou, Cheng Chi, Yibo Li, Jingkun An, Jiayuan Zhang, Shanyu Rong, Yi Han, Yuheng Ji, Mengzhen Liu, Pengwei Wang, et al. Robotracer: Mastering spatial trace with reasoning in vision-language models for robotics. *arXiv preprint arXiv:2512.13660*, 2025.
- [49] Muzhi Zhu, Hao Zhong, Canyu Zhao, Zongze Du, Zheng Huang, Mingyu Liu, Hao Chen, Cheng Zou, Jingdong Chen, Ming Yang, et al. Active-o3: Empowering multimodal large language models with active perception via grpo. *arXiv preprint arXiv:2505.21457*, 2025.